High Frequency Transformer Design Report
Work Package 4

OZAN KEYSAN
University of Edinburgh
June 12, 2014

Abstract

This report presents the material options for the core of the medium frequency transformer that is being investigated within the Work Package 4 of the "Next Generation HVDC Network for the OffshoreRenewable Energy Indusrty" project.

Keywords: medium frequency transformer, HVDC transmission, core losses, HV transformer

1 Introduction

A literature review is presented by Robert Fox within WP 2, in which different medium-frequency transformers were compared and the components of medium-frequency transformers are listed. This report will focus on the core materials and the main losses in a transformer.

Increasing frequency of a transformer reduces its volume and cost. In [1], it is stated that the weight and size of a 3 MW 1.2 kHz transformer is less than 8% of an equivalent 50 Hz line transformer. In Fig. 1, volume variation with operating frequency for a 1 MW transformer is presented.

However, as the frequency is increased, skin effect, proximity effect, hysteresis losses and dielectric losses are significantly increased. Furthermore, the reduction in size usually implies same power loss in much smaller area, which demands forced cooling. Important design factors in conventional line transformes and high frequency transformers are tabulated in Table 1. Challenges of medium-high frequency transformers can be listed as [2]:

- Loss reduction for higher frequency range.

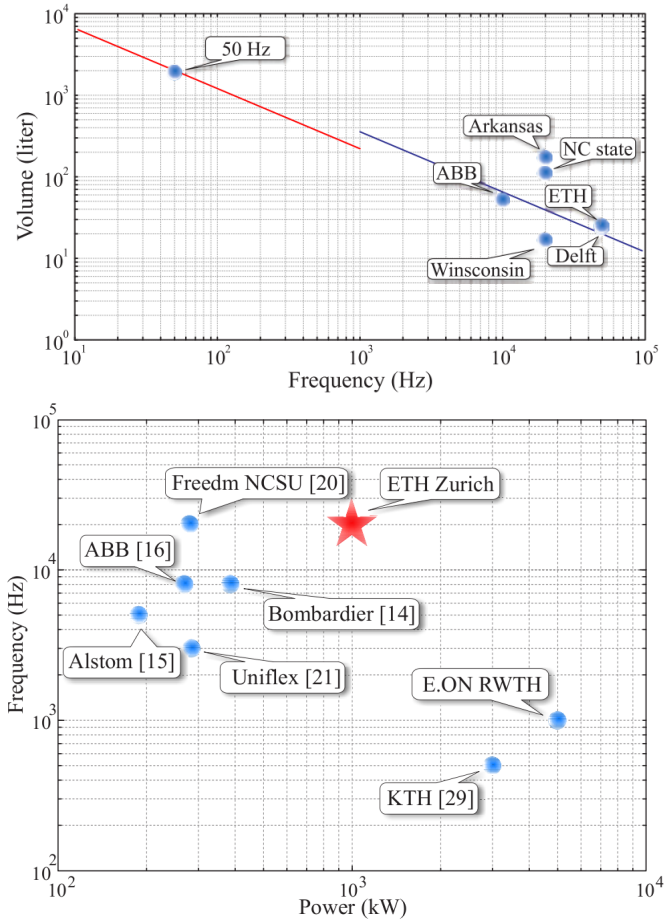

Figure 1: Volumes of high frequency transformers(normalized to 1 MW) and rated power and operating frequencies of existing DC-DC converter prototypes [3, 4].

- Efficient thermal management, higher power levels are contained in equal volumes.
- High-dielectric stress generated by rapidly changing rectangular voltage waveforms.
- High-isolation levels are required (due to multi-level inverter structure).
- Generation of acoustic noise, which reaches the most sensitive range of the human ear.

Line Transformer (50 Hz)	High Frequency Transformer
Core Mass	Skin Effect
Copper Losses	Core Losses
Volume	Parasitic Capacitance
	Cooling
	Resonance

Table 1: Important factors in the design of line frequency and high-frequency transformers.

2 Core Materials

Although, various types of electrical steel laminations are commonly used in power transformers. As the operating frequency is increased, there are more options available:

Amorphous Materials

Amorphous cores are typically made of Metglas (metalic glass alloy), which is a thin non-crystalline amorphous metal alloy of iron, boron, silicon and phosphorus. The material has a much higher resistivity in electrical steel which results in a low eddy losses. Furthermore, the hysteresis losses of amorphous cores are lower, which reduces the no-load losses compared to one with electrical steel. However, amorphous materials usually have lower saturation flux density compared to conventional iron-silicon electrical steel.

Some manufacturers of amorphous transformer cores can be listed as:

- Hitachi Metals (Powerlite)
- Vacuumschmelze (Vitrovac)
- Metglas
- Vijai Electricals

Although, amorphous materials are superior to electrical steel laminations, nano-crystalline materials are superior to amorphous materials with their lower cost and higher flux densities [5]. Nano-crystalline materials will be discussed in the next section. The specifications of amorphous and nano-crystalline materials are compared in Table 2. The only application that a amorphous material can be more advantageous is high-frequency single-ended forward converter topologies. For all other topologies, nano-crystalline materials are considered to be more suitable.

	Amorphous (Vitrovac)	Nano-crystalline (VitroPerm)
Saturation Flux Density	0.8 T	1.2 T
Losses (f= 20 kHz, B=0.2 T)	2 W/kg	1.4 W/kg
Max. Operating temperature	110 °C	120 °C
Curie temperature	365 °C	600 °C

Table 2: Comparison of amorphous (Vitrovac) and nano-crystalline (VitroPerm) materials [5].

Nano-crystalline

Nano-crystalline is a fairly new material that consists of approximately 80% of iron with the remaining is mixture of silicon, boron, carbon, nickel and other materials. This is a special type of amorphous material, which has superior magnetic characteristics, such as lower core loss and high permeability. Other specifications can be listed as [6]:

- Up to 50 % permeability than 80% nickel material (e.g. Supermalloy).
- High saturation flux density (1.2-1.5 T).
- High operating temperature up to 130 °C.
- Minimal change of magnetic characteristics with temperature.
- 17 % lighter than Nickel with a density of 7.3 g/cm^3.
- Stacking density up to 90 % can be achieved.

Some main manufacturers of nano-crystalline materials can be listed as:

- MK Magnetics
- Vacuumschmelze
- Hill-Tech

In this section, different types of nano-crystalline materials will be compared. Vacuumschmelze manufactures various soft magnetic nano-crystalline materials under the brand of VitroPerm.

VitroPerm

Nanocrystalline VitroPerm alloys are based on Fe with Si and B with Nb and Cu additives [7]. VitroPerm nano-crystalline alloys are optimized to combine highest permeability and lowest coercive field strength. The combination of

very thin tapes and the relatively high electrical resistance (1.1-1.2 $\mu\Omega m$) to ensure minimal eddy current losses and an outstanding frequency vs. permeability behaviour. Along with saturation flux density of 1.2 T and wide operational temperature range, these features combine to make VitroPerm superior in many aspects to commonly used ferrite and amorphous materials. Magnetization curves and B-H characteristics of VitroPerm materials are presented in Fig. 2.

VitroPerm has a wide range material options with different permeability scale as as shown in Fig. 3. The permeability of VitroPerm 500F is significantly higher than ferrite as shown in Fig. 4.

VitroPerm has also a high operating temperature compared to ferrite. The Curie temperature of VitroPerm alloys are 600 °C. Furthermore, the saturation flux density only reduces by 10% at 120 °C, which allows the core can be overloaded for short-amount of periods up to $180 - 200$ °C. The variation of permeability with temperature for VitroPerm is presented in Fig. 5.

Silicon-Steel

Silicon-steel is a popular choice in line frequency power transformers for its low cost and high-saturation magnetic induction. However, core losses of silicon-steel is high compared to other materials, which makes them unsuitable for medium frequency transformers. The core losses of material will be compared in the next section.

Ferrites

Ferrites have a low-loss density in very high-frequencies, which makes them a suitable material for high-frequency applications such as RF-filters and chokes. However, they have saturation flux density around 0.5 T, which increases the core volume and mass in high power applications.

Core Material Comparison

Different core materials and manufacturers are presented in Table 3. In Fig. 6, prototypes with common core materials are presented. It can be seen from the table that nano-crystalline and amorphous materials are the most suggested materials for medium frequency transformers that work between 1 kHz and 25 kHz.

The hysteresis losses and the core loss of different materials are compared in Fig. 7. Core losses are presented in Fig. 8. It can be seen that between 1 kHz and 10 kHz, the core loss of 0.3 mm silicon-steel laminations are 25

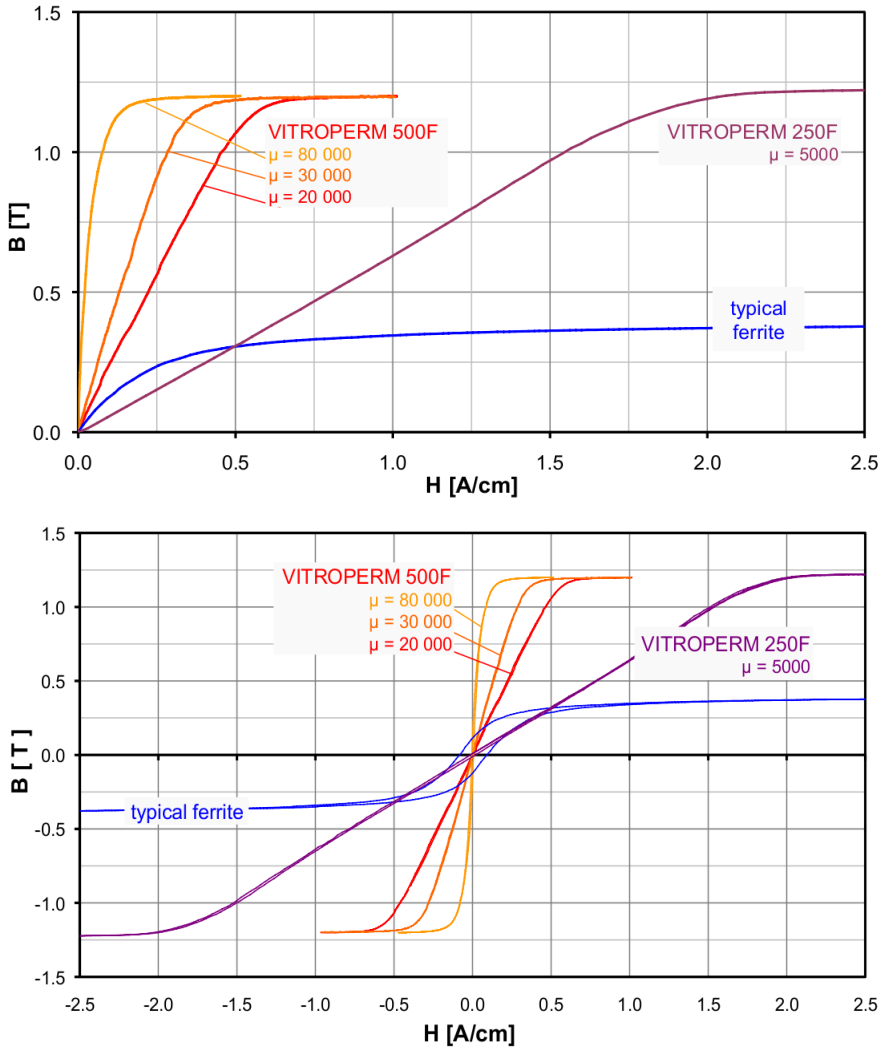

Figure 2: Magnetisation curve and B-H characteristics of VitroPerm [7].

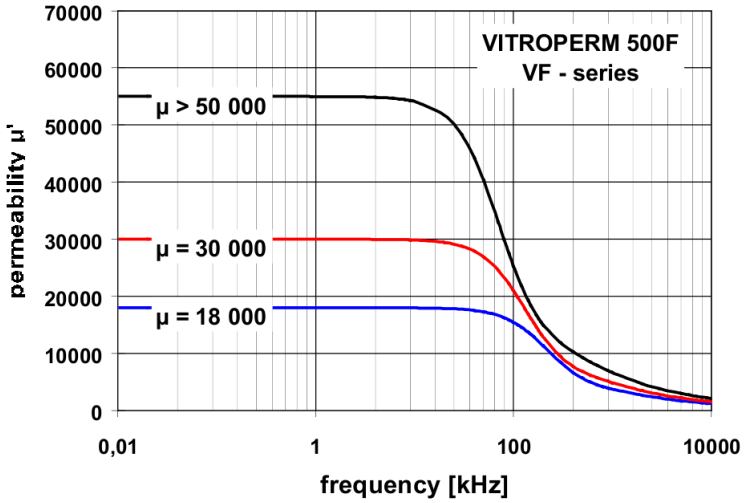

Figure 3: Permeability change of different VitroPerm materials with frequency [?].

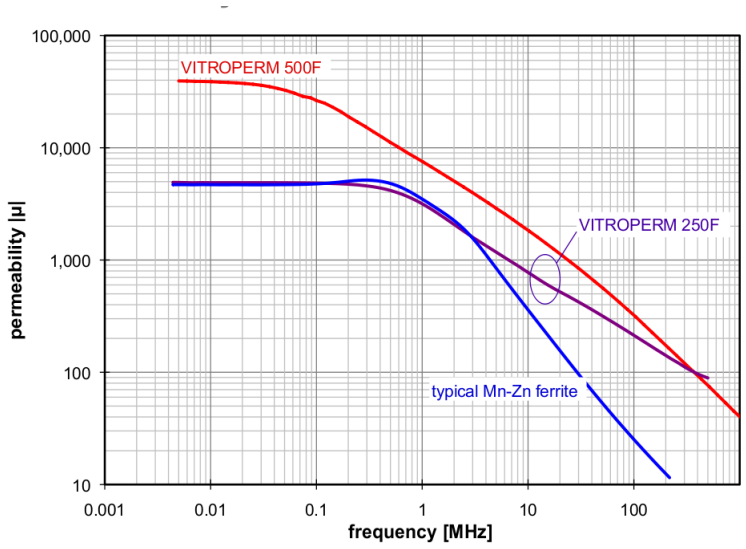

Figure 4: Permeability change of VitroPerm 250F($\mu = 5000$), VitroPerm 500F($\mu = 40000$) and ferrite($\mu = 5000$) with frequency. [7].

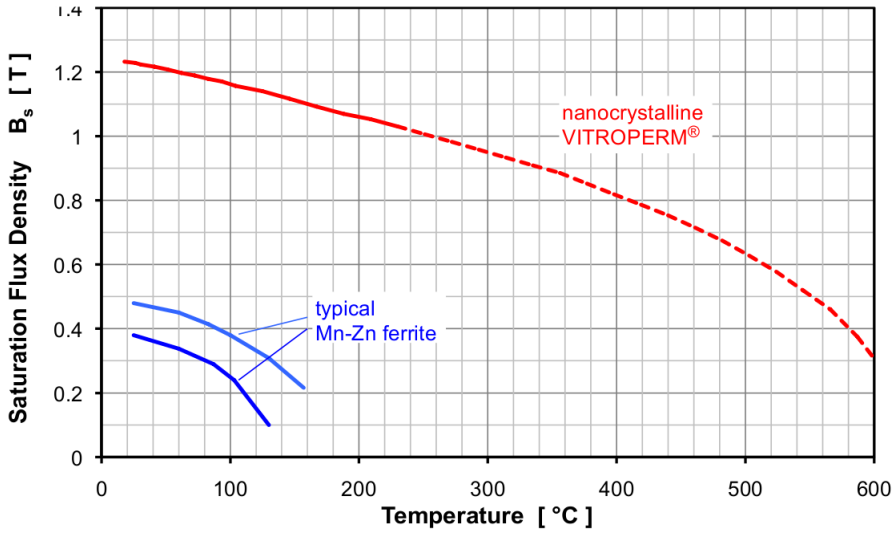

Figure 5: Saturation flux density variation of VitroPerm with temperature.

Material	Brand	Saturation Flux	Core Loss	Manufacturer
Amorphous	Microlite	1.56 T	1.5 kW/kg	Metglas
	Powerlite	1.56 T	0.6 kW/kg	Metglas
	Namglass	1.59 T	0.34 kW/kg	Magmet
	Vitrovac	0.82 T	0.19 kW/kg	VAC
Nano-crystalline	Finemet	1.23 T	0.14 kW/kg	Hitachi
	VitroPerm	1.2 T	0.07 kW/kg	VAC
	Nanoperm	1.2 T	0.04 kW/kg	Magnetec
	Namglass 4	1.23 T	0.04 kW/kg	Magmet
Silicon Steel	Arnon 7	1.53 T	1.6 kW/kg	Arnold
	Arnon 5	1.48 T	1.06 kW/kg	Arnold

Table 3: Core materials and manufacturers for high-frequency transmormers (specific losses at B = 1 T, f = 20 kHz) [4].

Frequency	Magnetic Material	Low-Leakage Inductance Resonant Converter	High-Leakage Inductance Non-Resonant Converter
< 1 kHz	**Silicon-Steel (FeSi)**		**Traction,** 75 **kVA** 400 Hz, Bare 340 µH, Oil [Hugo et al., 2007]
1 kHz to 25 kHz	**Nanocrystalline**	**Traction,** 350 **kVA** 10 kHz, Coaxial < 50 kg, 3 µH, Water [Heinemann, 2002]	**General,** 10 **kVA** 20 kHz, Litz wire 1.6 µH + L_{ext} 21 µH [Akagi and Inoue, 2006]
		Traction, 500 **kW** 8 kHz, Coaxial 2.3 µH, Water, 18 kg [Steiner and Reinold, 2007]	***Traction,*** 1 ***MVA*** *4 kHz, Litz wire* *215 µH, 148 kg, Cyclo* [Kjellqvist et al., 2004]
	Amorphous	**General,** 50 **kW** 25 kHz, Interleaved Foils 3 µH + L_{ext} 37 µH [Pavlovsky et al., 2005]	***Wind,*** 280 ***kVA*** *1.2 kHz, Coaxial* *251 nH, Passive Rectifier* [Prasai et al., 2008]
			Wind, 1 ***MW*** *10 kHz, HV Litz wire* *50 µH, Passive Rectifier* [Morren et al., 2001]
> 25 kHz	**Ferrite**		**Wind,** 3.6 **kW** 50 kHz, Litz wire 14 µH, Passive Rectifier [Morren et al., 2001]
			General, 50 **kW** 50 kHz, Coaxial 1.6 µH [Kheraluwala et al., 1992]
			Drives, 25 **kW** 50 kHz, Litz wire 2.2 mH, Forced Air [Aggeler et al., 2008]

Figure 6: Common materials used in medium frequency transformers and previous prototypes (Heinemann, 2002:[8], Steiner,2007:[9], Pavlovsky,2005:[10], Morren,2002:[11], Prasai,2007:[1]) [2].

times higher than nano-crystalline material. A 50 kV, high frequency (20 kHz), 150 kW transformer that uses nano-crystalline material is presented in [12], in which the core losses are estimated as 60W/kg at an operating flux density of 1 T.

3 Losses in a Transformer

3.1 AC Winding Losses

The high frequency excitation in a medium frequency transformer has two main effects in the transformer windings:

- Skin Effect: In AC excitation the current itself generates an opposing magnetic field and current, which reduce the net current density inside the conductor. The total current will stay same, but the distribution will be higher across the circumference of the conductor.
- Proximity Effect is the interaction between two adjacent conductors that alters the current distribution in the conductor. Same principles(e.g. proximity, frequency) apply in the proximity affect.

3.1.1 Skin Effect

Skin effect is an important factor in AC resistance and eddy current losses in a transformer. Skin effect is effected by the skin depth, which can be expressed as:

$$\sigma = \sqrt{\frac{2\rho}{\mu\omega}} \tag{1}$$

where ρ is the resistivity of the conductor, μ is permeability, and ω is the frequency in rad/s. Skin depth of copper for different operating frequencies are presented in Table 4. For reasonable AC resistance characteristics, the rule of thumb is to choose the conductor diameter smaller than 1.6 times of the skin depth. Thus, for a 1-2 kHz transformer application, the conductor should not be thicker than 2-3 mm.

In a step-up transformer the cross-section area of the primary conductor will be larger. However, the limit due to skin-depth limits the thickness of the conductor. Therefore, the most feasible way is to use foil conductors in the primary windings. Dowell calculated eddy losses in foil type transformer windings in [13]. A detailed explanation of these one dimensional Maxwell equations can be found in [2] and a summary will be presented in this section.

The DC resistance of a foil winding can be expressed as:

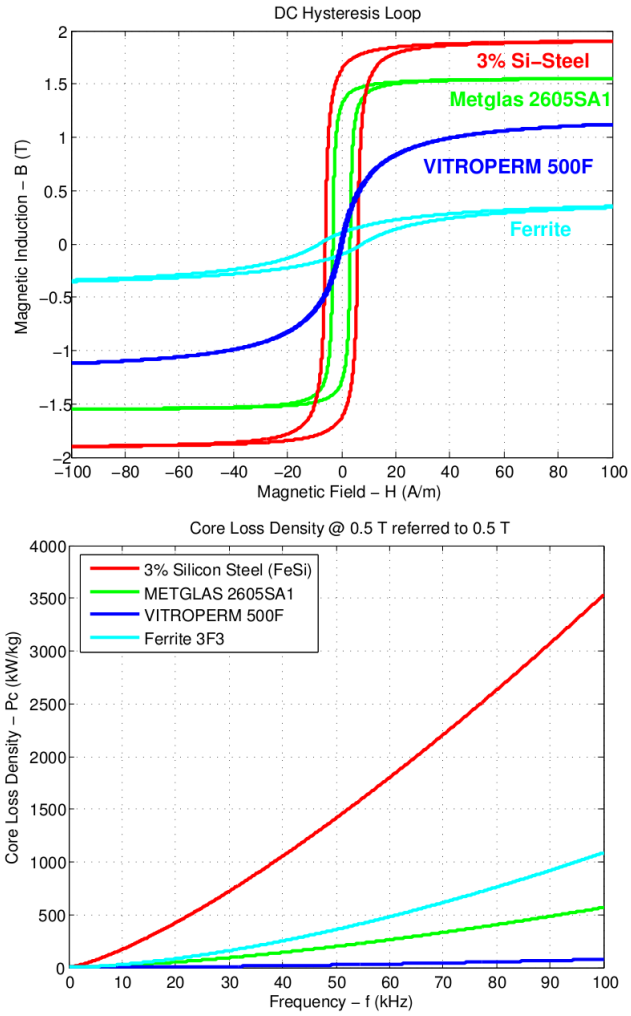

Figure 7: Loss comparison of silicon-steel, amorphous, nano-crystalline and ferrite materials [2]. a) Hysteresis loss, b) Core loss.

Frequency	Skin Depth
50 Hz	9.2 mm
1 kHz	2.06 mm
2 kHz	1.49 mm
5 kHz	0.94 mm
10 kHz	0.65 mm
50 kHz	0.29 mm

Table 4: Skin depth in a copper conductor.

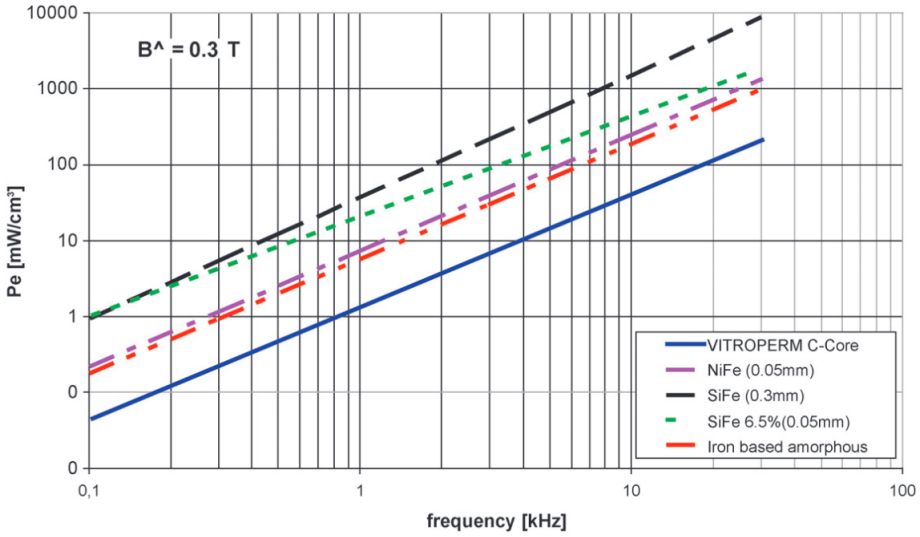

Figure 8: Core loss comparison of nano-crystalline (VitroPerm) with electrical steel and amorphous material [7].

$$R_{dc} = \rho \frac{L_{mean}}{t_w h_w} N_{turns} \tag{2}$$

where L_{mean} is the mean turn length of the coil, t_w is the thickness, h_w is the height, ρ is the resistivity of copper.

The AC resistance is more complicated to calculate and depends on the ratio of the wire thickness to skin depth (δ) and can be expressed as:

$$R_{ac} = \rho \frac{L_{mean}}{h_w \delta} N_{turns} \left[\varsigma_1 + \frac{2}{3}(N_{turns}^2 - 1)\varsigma_2 \right] \tag{3}$$

where:

$$\varsigma_1 = \frac{sinh(2\Delta) + sin(2\Delta)}{cosh(2\Delta) - cos(2\Delta)} \quad \varsigma_2 = \frac{sinh(\Delta) - sin(\Delta)}{cosh(\Delta) + cos(\Delta)} \quad \Delta = \frac{t_w}{\delta} \tag{4}$$

as can be seen from the equation above, the important factor is the penetration factor (i.e the ratio of conductor thickness to skin depth, Δ). The ratio of AC resistance to DC resistance is called Dowell's resistance factor (F_r). The resistance factor as a function of penetration ratio for a 2 mm thick foil wire is presented in Fig. 9. For example, at 1 kHz the skin depth is 2.1 mm (the penetration ratio is approximately 1), the resistance factor is 2.7 for a layer number of 4. Thus the resistive losses will be 2.7 times more compared to DC conduction.

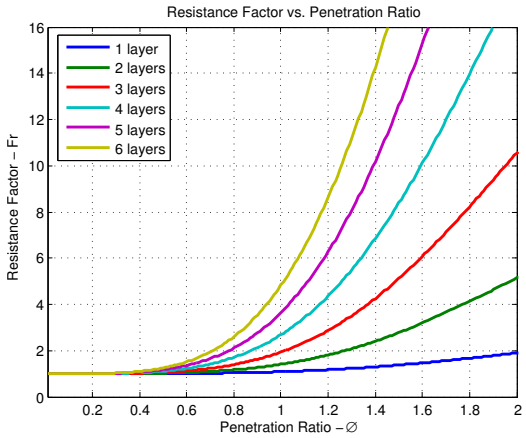

Figure 9: Resistance factor for a function of penetration ratio (for 2 mm thick foil conductor) [2].

3.1.2 Secondary-Winding

There are different analytical models to estimate the AC resistance in round conductors (e.g. high voltage cables that can be used in the secondary winding), such as presented in [14, 15]. Although, the method presented by Dowell in [13] is assumed as the most established method. In this method Dowell introduced a porosity factor to convert the round conductors to square conductors and then convert to foil type conductors.

Equivalent thickness of a round conductor can be defined as [13]:

$$\mathrm{d}_w = \sqrt{\frac{\pi}{4}} d \quad (5)$$

where d is the diameter of the round conductor and d_w is the thickness of the equivalent square conductor. Then, similar technique can be applied to convert square conductor to foil type conductor using a second porosity factor as shown in [2]. Therefore, the AC resistance of the round conductor can be expressed similarly to equation (3)) as given in [2].

4 Core Losses

The core losses mainly depend on the material type, flux density and operating frequency. The most common way to estimate the core losses is to use a power equation, which is known as the Steinmetz equation:

$$P_{core} = K f^a B^b \quad (6)$$

where K is a factor depending on the characteristic of the material, f is the operating frequency, B is the operating magnetic flux density, a and b are determined by the material characteristic obtained from the manufacturer's data.

Steinmetz equation is usually well establied method for line transformers, in which sinusoidal excitation is used. However, in the medium-high frequency transformers, the transformer is excited using power electronics (usually a square waveform, or stepped waveform), and transformer voltage and current include many harmonics.

For non-sinusoidal waveforms, the easiest way to calculate the core losses is to use Fourier transform to get the frequency components and then to estimate individual core losses for each component. There are more deteiled models as reviewed in [2]:

- Modified Steinmetz Equation
- Improved Generatlized Steinmetz Equation
- Equicalent Elliptical Loop
- Waveform Coefficient Steinmetz Equation

Although these methods can provide more accurate results compared to Fourier transform method, they all require extra measurement steps to determine the material characteristics at different operating frequenciues and waveforms. Therefore, it is impractical to use these models without experimental study at first. Therefore, using standard Steinmetz equation with harmonics contents is an ideal choice for analytical core loss estimation.

4.1 Core Losses in Non-Sinusoidal Excitation

The transformer developed by Narec will be excited using a square waveform in the low voltage side, and a multi-level inverter will be used in the high voltage side.

The core losses resulting from the low-voltage square wave excitation can be calculated by expressing the square wave as a Fourier series:

$$f(x) = \frac{4}{\pi} \sum_{n=1,3,5...}^{+\infty} \frac{1}{n} sin(n\omega x) \tag{7}$$

where ω is the frequency of the square waveform in radians/s, n is the harmonic order. The magnitudes of the Fourier series components of the square wave relative to the magnitude of the square wave is presented in Table 4.1.
Fourier series magnitudes relative to the magnitude of the square wave.

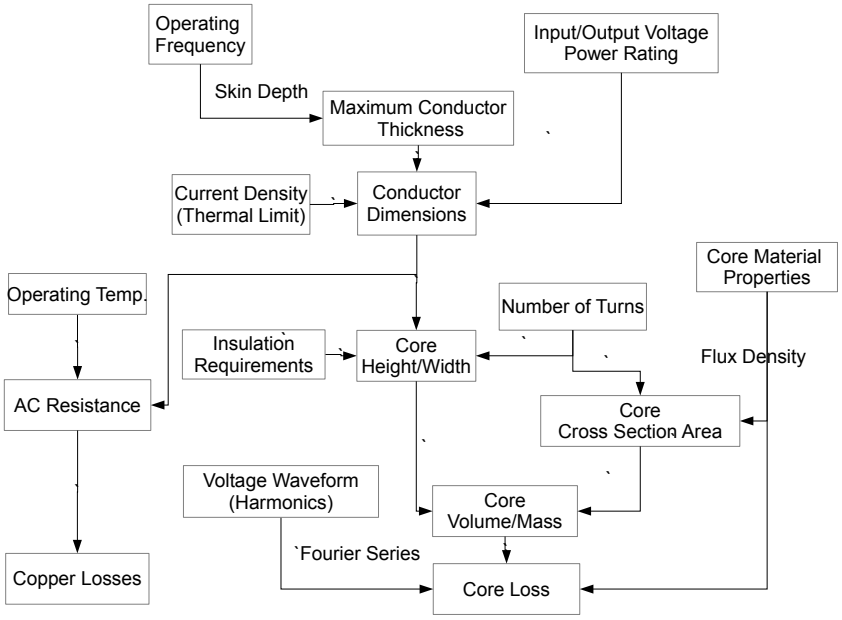

Figure 10: Design methodology to estimate transformer parameters and losses.

kablo katalogu http://dielectricsciences.thomasnet.com/viewitems/all-categories/wire-cable-2

5 Modelling of the Transformer

A Matlab model is developed to estimate the transformer models and calculate copper and core losses. The design methodology used in the Matlab code is depicted in Fig. 10.

5.1 Estimation of Winding Parameters

It is assumed from the WP 2 report that, foil type conductors are the most suitable option for the low voltage side. On the high voltage side, circular stranded cables are more suitable with their mechanical strength and increased dielectric insulation.

The thickness of the coil is chosen according to the skin depth at the operating frequency. The conductor thickness is selected to be less than 1.5 times skin depth, however, actual foil conductor thicknes is limited to standard wire gauges (e.g. 1 mm, 1.6 mm, 2 mm, 2.25 mm...). The frequency of the transformer versus the most suitable foil coil thickness is plotted in

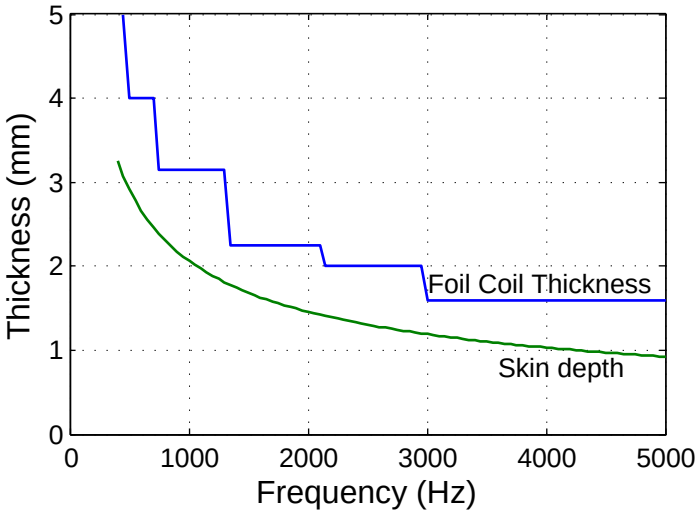

Figure 11: Skin depth and primary foil winding size variation (Standard foil conductor sizes are used).

Fig. 11. FOr example, for operating frequencies between 2 kHz and 3 kHz, the most suitable conductor thickness is 2 mm.

Then, using rated current and the rated current density, the required conductor area can be calculated. The conductor height can be found by dividing the conductor area to conductor thickness. For example, assuming a current density of $4A/mm^2$, the foil conductor height can be calculated as a function of the operating frequency as shown in Fig. 12.

The insulation parameters should be known to determine the dimensions of the primary and secondary windings. Dry insulation is considered to be the most suitable insulation type due to increased reliability and ease of manufacturing. However, oil flooded windings can be prefered to improve thermal performcance.

In the graphs below following arbitrary insulation thickness values are used, which can be modified for a more accurate estimation.

- Insulation thickness between primary (low voltage) conductors: 1 mm
- Insulation thickness from primary winding to core: 10 mm
- Outer insulation thickness around primary winding: 10 mm
- Insulation thickness between secondary (high voltage) conductors: 5 mm
- Insulation thickness from secondary winding to core: 20 mm
- Outer insulation around secondary winding: 20 mm

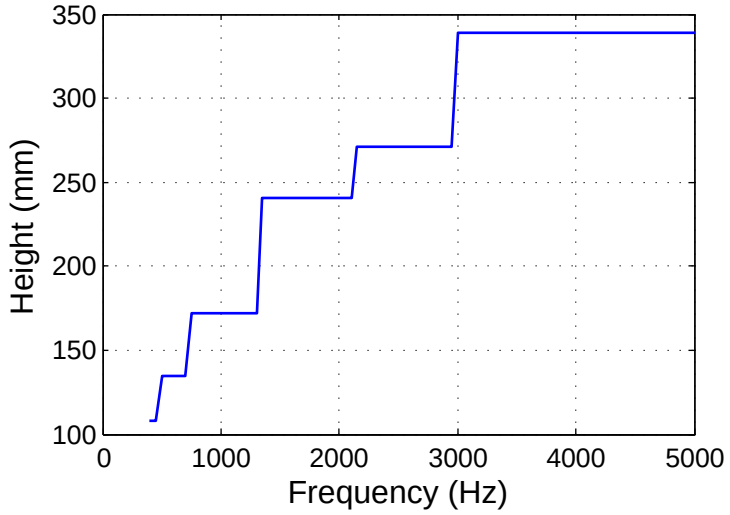

Figure 12: Height of the foil conductor as a function of the operating frequency.

- Insulation thickness between primary and secondary windings: 50 mm

5.2 Estimation of Core Dimensions

The most important parameter of the core is the cross-section area, which depends on the operating frequency, flux density in the core and the number of turns. Assuming a square cross-section area, the thickness of the core as a function of the primary number of turns is estimated as in Fig. 13, and similarly graphs for the secondary number of turns are presented in Fig. 14. The operating flux density of the core is assumed as 1.1 T, the primary voltage magnitude is assumed as 3 kV, and the secondary voltage magnitude is assumed as 300 kV.

Core mass calculations to be added.

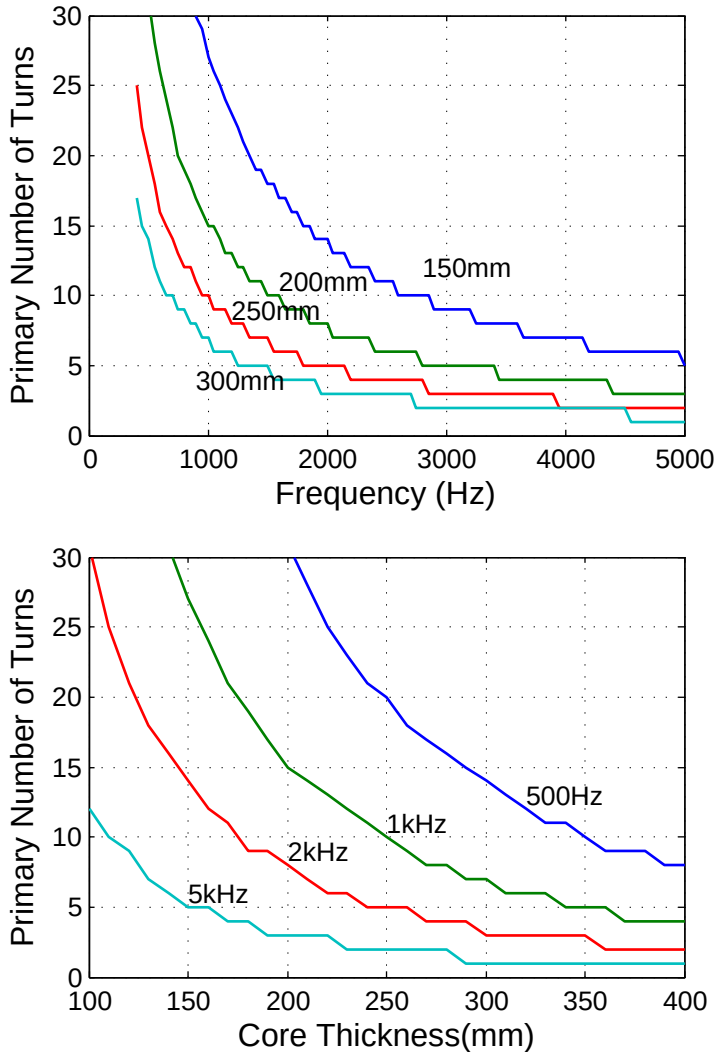

Figure 13: Core-thickness (assuming square cross-section area) as a function of the primary number of turns and operating frequency (B=1.1 T, Vin=3 kV, Vout=300 kV).

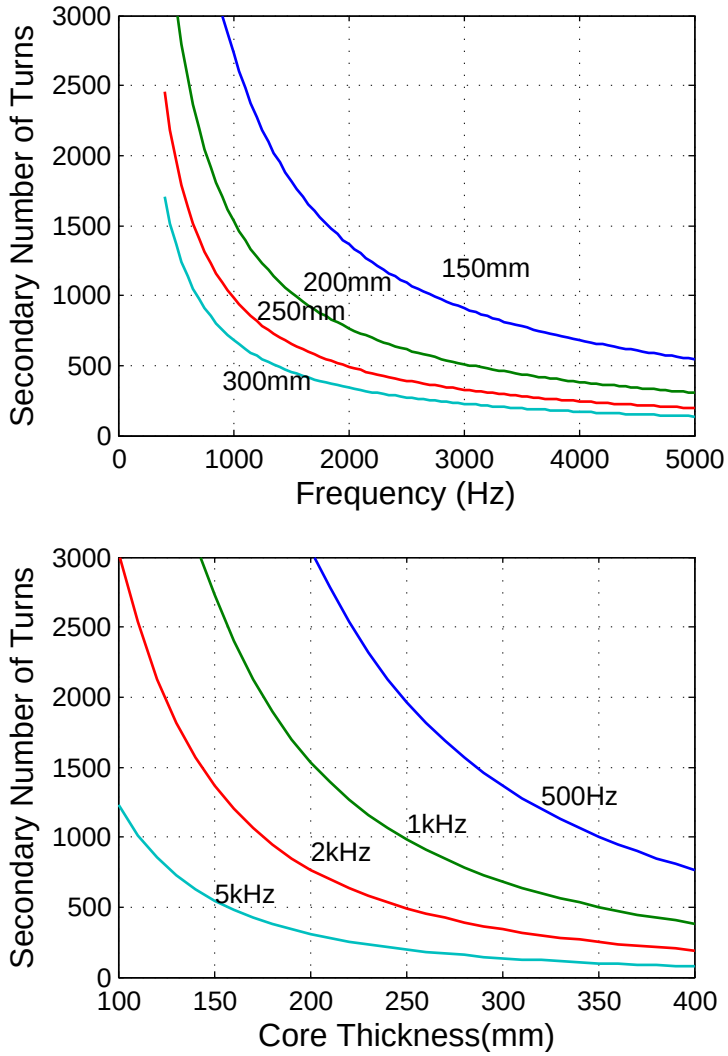

Figure 14: Core-thickness (assuming square cross-section area) as a function of the secondary number of turns and operating frequency (B=1.1 T, Vin=3 kV, Vout=300 kV).

References

1. Anish Prasai, Deepak Divan, Ashish Bendre, and Frank Kreikebaum. A new architecture for offshore wind farms. In *2007 European Conference on Power Electronics and Applications*, pages 1–10. IEEE, 2007.
2. Irma Villar. *Multiphysical characterization of medium-frequency power electronic transformers*. Phd dissertation, École Polytechnique Federale de Lausanne, 2010.
3. G Ortiz, J Biela, D Bortis, and J. W. Kolar. 1 Megawatt, 20 kHz, isolated, bidirectional 12kV to 1.2kV DC-DC converter for renewable energy applications. In *The 2010 International Power Electronics Conference - ECCE ASIA -*, pages 3212–3219. IEEE, June 2010.
4. G. Ortiz, J. Biela, and J. W. Kolar. Optimized design of medium frequency transformers with high isolation requirements. In *IECON 2010 - 36th Annual Conference on IEEE Industrial Electronics Society*, pages 631–638. IEEE, November 2010.
5. Vacuumschmelze. Vitroperm 500 F - VitroVac 6030 F. Technical report.
6. MK Magnetics. Nanocrystalline: A Special Product Announcement.
7. Vacuumschmelze. Nanocrystalline VITROPERM. Technical report.
8. Lothar Heinemann. An actively cooled high power, high frequency transformer with high insulation capability. In *APEC. Seventeenth Annual IEEE Applied Power Electronics Conference and Exposition (Cat. No.02CH37335)*, volume 00, pages 352–357. IEEE, 2002.
9. Michael Steiner and Harry Reinold. Medium frequency topology in railway applications. In *2007 European Conference on Power Electronics and Applications*, pages 1–10. IEEE, 2007.
10. M Pavlovsky, S.W.H. de Haan, and J.A. Ferreira. Concept of 50 kW DC/DC converter based on ZVS, quasi-ZCS topology and integrated thermal and electromagnetic design. In *2005 European Conference on Power Electronics and Applications*, pages 9 pp.–P.9. IEEE, 2005.
11. J Morren, SWH de Haan, and JA Ferreira. High-voltage DC-DC converter for offshore windfarms. *IEEE Young Researchers Symposium in Electrical Power Engineering*, pages 1–6, 2002.
12. T Filchev, J Clare, P Wheeler, and R Richardson. Design of high voltage high frequency transformer for pulsed power applications. In *IET European Conference on European Pulsed Power 2009. Incorporating the CERN Klystron Modulator Workshop*, pages P18–P18. IET, 2009.
13. P.L. Dowell. Effects of eddy currents in transformer windings. *Proceedings of the Institution of Electrical Engineers*, 113(8):1387, 1966.

14. X Nan and C.R. Sullivan. An improved calculation of proximity-effect loss in high-frequency windings of round conductors. In *IEEE 34th Annual Conference on Power Electronics Specialist, 2003. PESC '03.*, volume 2, pages 853–860. IEEE, 2003.

15. J.a. Ferreira. Improved analytical modeling of conductive losses in magnetic components. *IEEE Transactions on Power Electronics*, 9(1):127–131, 1994.